

# Magnetic Field Analysis of a Delta-Connected Autotransformer Based 18 Pulse AC-DC Converters

Arafet Ben Ammar<sup>#1</sup>, Faouzi Ben Ammar<sup>\*2</sup>

<sup>#</sup>Université de Tunis, ENSIT,  
Laboratoire matériaux, Mesures  
et Applications MMA, INSAT

<sup>1</sup>arafet.ammar@hotmail.fr

<sup>\*</sup>Université de Carthage, INSAT,  
Laboratoire matériaux, Mesures  
et Application MMA, INSAT

<sup>2</sup>faouzi.benamar@yahoo.fr

**Abstract**—To improve the total harmonic distortions (THD) of input line currents, the authors present the design of the Delta-connected three phase autotransformer based 18 pulse AC-DC converter. The proposed work takes account the magnetic core topology and the winding position. Moreover, advanced numerical techniques, based on the two-dimensional (2D) and three-dimensional (3D) finite element method (FEM), have been applied for the magnetic field analysis of power transformer (the flux density, the field density, the current density and flux lines). Experimental validation of the proposed methodology is also provided.

**Keywords**— autotransformer; Design; 2D, 3D finite element modeling.

## I. INTRODUCTION

The thyristor AC-DC converter structure 6-pulse is widely used in industry for various applications. The total harmonic distortions (THD) of input line currents of the six-pulse rectifier can reach 31%. In order to meet the harmonic requirement set by IEEE standard 519-1992 [1], the multi-pulse rectifiers 12, 18 and 24 are adopted to insure that any individual harmonics should not be more than 3% and total harmonic distortion (THD) should not be more than 5%. In order to eliminate 5<sup>th</sup>, 7<sup>th</sup> harmonics in the network side, the 12 pulse rectifier is realized by a serial connection of two 6-pulse rectifier [3]-[5], the first rectifier is fed by an YY connected transformer, while the second rectifier is fed by an Δ-Y connected transformer to introduce the 30° phase shift. The AC-DC 18 pulse rectifier is realized with three 6-pulse rectifier in order to eliminate the 5<sup>th</sup>, 7<sup>th</sup>, 11<sup>th</sup> and 13<sup>th</sup> harmonics. The 18 pulse structure requires the design of auto-transformer with special couplings. Various configurations of auto-connected transformers for an 18-pulse AC-DC converter are proposed [2]-[6]. This paper is organized as follow; section II gives a mathematical description of the various winding current, voltages and capacity delta-connected autotransformer-based 18-pulse AC-DC converter with 40° phase shifting of reduced harmonic. Section III gives magnetic field analysis and geometry design of the proposed autotransformer. Moreover, section IV gives an advanced

numerical technique, based on 2D and 3D finite element method (FEM) using Maxwell ANSYS, for the magnetic field analysis of power transformer (the flux density, the field density, the current density and flux lines) and the mesh operations [7]-[12]. Finally in section V the simulation results of the topology of 18-pulse are discussed and validated in experimental realization.

## II. ANALYSIS AND DESIGN OF THE PROPOSED AUTOTRANSFORMER

The Delta-connected autotransformer is designed where it is supplied by three-phase input voltage ( $V_a, V_b, V_c$ ) displaced at 120° with respect to each other, it produces from sets of balanced three-phase voltages, namely ( $V_{11}, V_{12}, V_{13}$ ) and ( $V_{21}, V_{22}, V_{23}$ ), all displaced through an angle +40° and -40° desired for the 18-pulse converter operation shown in Fig.1.

$$V_{11} = V_a - K_1 \cdot V_{ac} - K_2 \cdot V_{bc} \quad (1)$$

$$V_{21} = V_a - K_1 \cdot V_{ab} + K_2 \cdot V_{bc} \quad (2)$$

$K_1, K_2$  and  $K_3$  are the measures of turn's ratios of the various windings of the auto-connected transformer

Assume the following set of voltages:

$$V_1 = V[0^\circ], V_2 = V[-120^\circ], V_3 = V[120^\circ] \quad (3)$$

$$V_{11} = V[40^\circ], V_{12} = V[-80^\circ], V_{13} = V[160^\circ] \quad (4)$$

$$V_{21} = V[-40^\circ], V_{22} = V[-160^\circ], V_{23} = V[80^\circ] \quad (5)$$

Where:

$$K_1 = 0.1559, K_2 = 0.293 \text{ and } K_3 = 0.6882$$

Under of the assumption of idealized circuit conditions, ideal transformers and the constant current  $I_{dc}$ , the systems solution can acquire from Kirchhoff's law current and the balance conditions of the ampere-turns of each transformer limbs.

In the connection depicted in Fig. 1 and Fig.2, Kirchhoff's current law can be written as follows [6]:

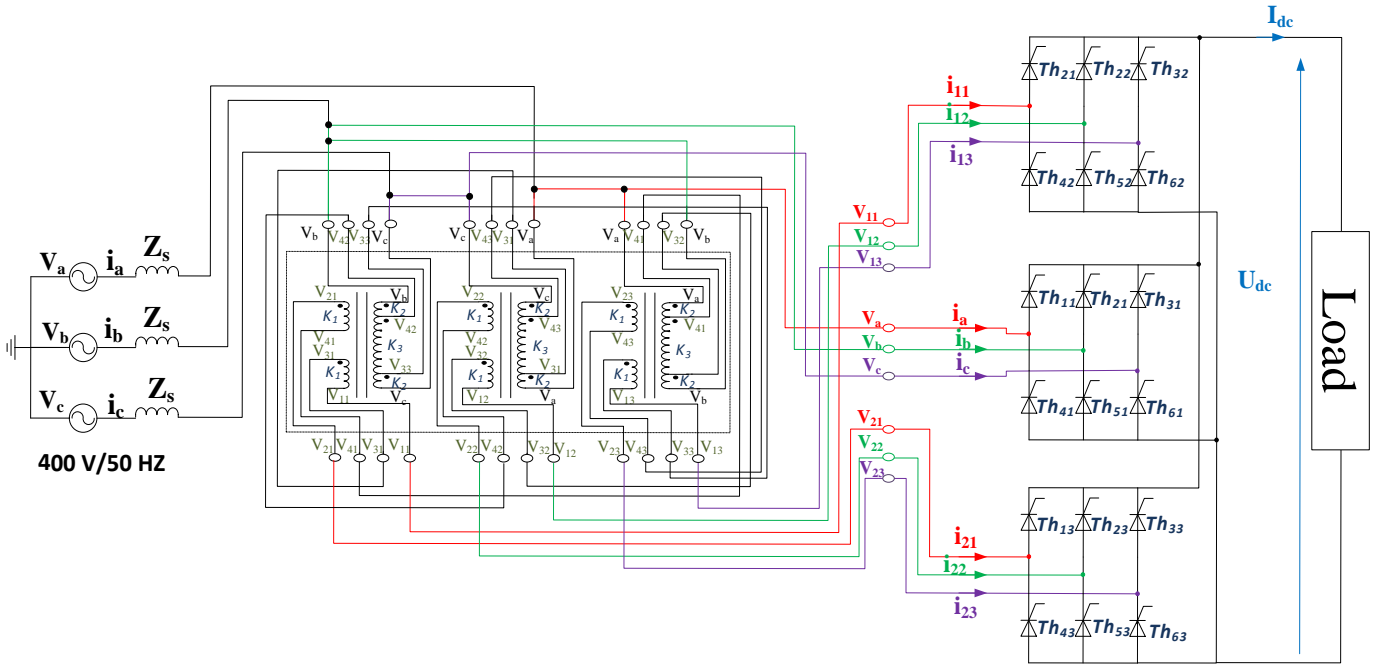


Fig. 1 Autotransformer based 18-pulse ac-dc converter

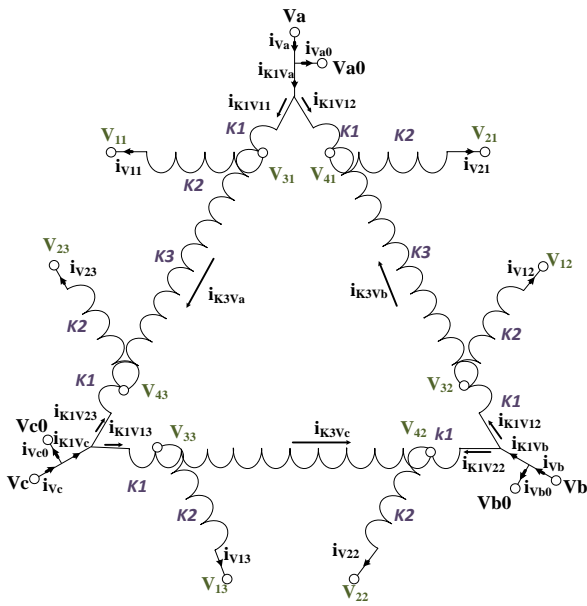


Fig. 2 Autotransformer winding connection

For phase  $V_a$ :

$$\begin{aligned} i_{V_a} &= i_{V_{a0}} + i_{K1V_a} \\ i_{K1V_a} &= i_{K1V_{11}} + i_{K1V_{21}} \\ i_{K1V_{11}} &= i_{V_{11}} + i_{K3V_a} \\ i_{K1V_{21}} &= i_{V_{22}} - i_{K3V_b} \end{aligned} \quad (6)$$

For phase  $V_b$ :

$$\begin{aligned} i_{V_b} &= i_{V_{b0}} + i_{K1V_b} \\ i_{K1V_b} &= i_{K1V_{12}} + i_{K1V_{22}} \end{aligned} \quad (7)$$

$$i_{K1V_{12}} = i_{V_{12}} + i_{K3V_b} \quad (12)$$

$$i_{K1V_{22}} = i_{V_{22}} - i_{K3V_c} \quad (13)$$

For phase  $V_c$ :

$$i_{V_c} = i_{V_{c0}} + i_{K1V_c} \quad (14)$$

$$i_{K1V_c} = i_{K1V_{13}} + i_{K1V_{23}} \quad (15)$$

$$i_{K1V_{13}} = i_{V_{13}} + i_{K3V_c} \quad (16)$$

$$i_{K1V_{23}} = i_{V_{23}} - i_{K3V_a} \quad (17)$$

The ampere-tours equations of the autotransformer are expressed as follows:

$$K_2(i_{V_{11}} - i_{V_{21}}) + K_1(i_{K1V_{22}} - i_{K1V_{13}}) - K_3i_{K3V_c} = 0 \quad (18)$$

$$K_2(i_{V_{12}} - i_{V_{22}}) + K_1(i_{K1V_{23}} - i_{K1V_{11}}) - K_3i_{K3V_a} = 0 \quad (19)$$

$$K_2(i_{V_{13}} - i_{V_{23}}) + K_1(i_{K1V_{21}} - i_{K1V_{12}}) - K_3i_{K3V_b} = 0 \quad (20)$$

The currents,  $i_{V_{a0}}$ ,  $i_{V_{11}}$ ,  $i_{V_{21}}$ ,  $i_{V_{b0}}$ ,  $i_{V_{12}}$ ,  $i_{V_{22}}$  and  $i_{V_{c0}}$ ,  $i_{V_{13}}$ ,  $i_{V_{23}}$  are obtained from the conduction conditions of the corresponding thyristor. The solutions of current related phase  $V_a$  are expressed as follows:

$$i_{K3V_a} = K_2(i_{V_{12}} - i_{V_{22}}) + K_1(i_{V_{23}} - i_{V_{11}}) \quad (21)$$

$$i_{K3V_b} = K_2(i_{V_{13}} - i_{V_{23}}) + K_1(i_{V_{21}} - i_{V_{12}}) \quad (22)$$

$$i_{K3V_c} = K_2(i_{V_{11}} - i_{V_{21}}) + K_1(i_{V_{22}} - i_{V_{13}}) \quad (23)$$

Consequently, the autotransformer winding currents and the line currents are obtained by substituting equations (21) - (22) into (6) - (17).

The total autotransformer capacity is expressed by:

$$S_T = 6K_2V_l I_{V_{11}} + 6K_1V_l I_{K1V_{11}} + 3K_3V_l I_{K3V_a} \quad (24)$$

$$S_T = 1210.70 I_{DC} \quad (10)$$

$$(11)$$

The autotransformer total equivalent capacity is defined by

$$S_{t,equiv} = \frac{1}{2} \frac{S_T}{V_{dc} I_{dc}} \quad (25)$$

Where  $V_l$  is the rms value of the line-to-line voltage of the power source,  $V_{dc}$  and  $I_{dc}$  are the average values of the dc output voltage and current, respectively.

The rms values of currents are given by

$$I_{K3Va} = \frac{\sqrt{2}}{3} I_{DC} \sqrt{(K_2 - K_1)^2 + K_2^2 + K_1^2} \quad (26)$$

$$I_{K3Va} = 0.169 I_{DC}$$

$$I_{K1V11} = \frac{I_{DC}}{3} \sqrt{(1 + K_2 - K_1)^2 + 2K_2^2 + (K_2 - K_1)^2 + b^2 + (1 - K_1)^2} \quad (27)$$

$$I_{K1V11} = 0.711 I_{DC}$$

$$I_{V11} = \frac{\sqrt{3}}{2} I_{DC} \quad (28)$$

$$I_{V11} = 0.866 I_{DC}$$

The THD current is calculated by the relationship between the rms value of line current and the effective value of the fundamental frequency component of the line current. These values are obtained by analyzing the waveform of the current [5].

$$I_{Va} = \sqrt{\frac{1}{2\pi} \int_0^{2\pi} I_{Va}(t)^2 d\omega t} \quad (29)$$

$$I_{Va1} = \sqrt{\frac{1}{2\pi} \int_0^{2\pi} I_{Va1}(t)^2 d\omega t} \quad (30)$$

$$THD = \sqrt{\frac{I_{Va}^2 - I_{Va1}^2}{I_{Va1}^2}} \quad (31)$$

### III. MAGNETIC FIELD ANALYSIS

Finite Element modelling (FEM) is a highly accurate method of calculating the transformer parameters. The FEM formation makes use of the fact that partial-differential equation is satisfied when total magnetic energy function is a minimum [7].

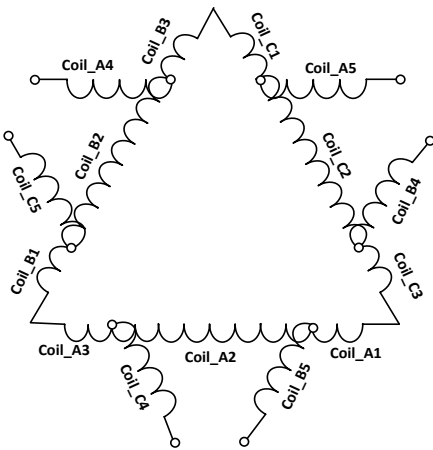


Fig. 3 Coil names

The geometry to solve (which is basically the core and set of transformer winding represented simple as rectangular blocks) can be drawn using the Maxwell ANSYS when we do a cross section. The appellations of coils shown in Fig. 3 are Coil\_A<sub>n</sub>, Coil\_B<sub>n</sub>, Coil\_C<sub>n</sub> (n=1:5) respectively for the phase A, phase B and phase C. Each limb has five concentrates coils to improve the magnetic coupling between the coils. The design of the limbs and core considered phase A are shown in Fig. 4. The Table 1 and Table 2 shows respectively the geometrical parameters of core and coils.

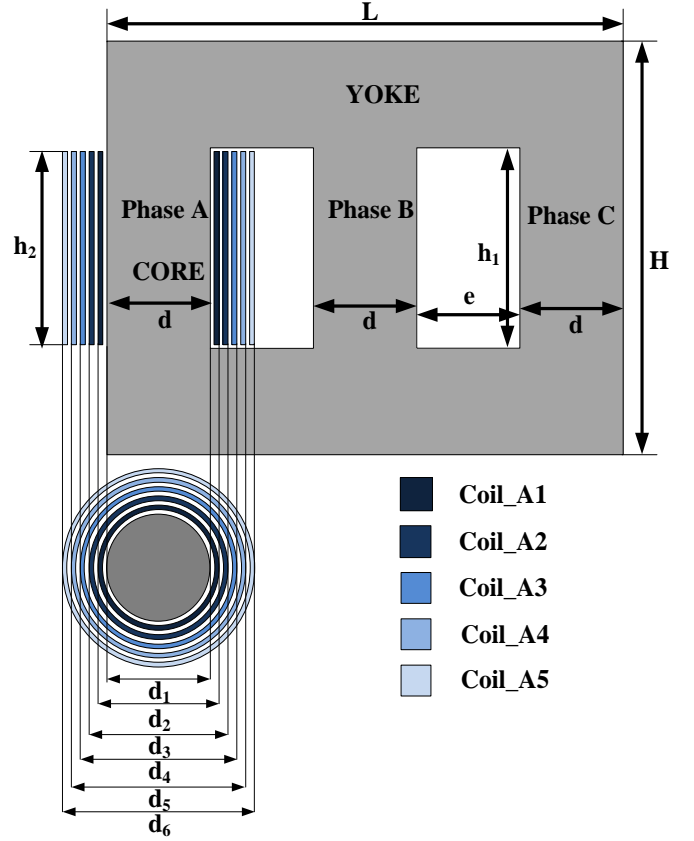


Fig. 4 Three limbs, three phase core and coil type autotransformer

TABLE I  
CORE PARAMETERS GEOMETRY

Geometry design				
H	L	d	e	h <sub>1</sub>
200mm	200mm	40 mm	40 mm	120mm

TABLE III  
COIL PARAMETERS GEOMETRY

Geometry design						
Coil_A (mm)						
d <sub>1</sub>	d <sub>2</sub>	d <sub>3</sub>	d <sub>4</sub>	d <sub>5</sub>	d <sub>6</sub>	h <sub>2</sub>
40	47	51	55	59	63	119

Selection of steel is important to determine the number of turns of each coil. The magnetic performance of steel is dominated by its Carbon content, for example the steel grade AISI 1010 content less than 0.1% Carbon. According to BH curve Fig.5, the relationship becomes highly nonlinear at  $B \geq 1.5$  Tesla and the material exhibits fully saturable behaviour at

$B \geq 2$  Tesla. The fully saturated behaviour is reached when the material permeability  $\mu = \frac{\Delta B}{\mu_0 \Delta H} \cong 1$  [8]. Eddy current losses within a transformer are reduced and controlled by reducing the thickness of the steel core. These laminations are insulated from each other by a covering of varnish or paper to increase the resistivity of the core thus increasing the overall resistance to limit the flow of the eddy currents.

The Turn number of each coil of the autotransformer is calculated using Boucherot theorem as shown in Table 3.

$$N_{coil} = \frac{V_n \cdot 10^8}{4.44 f B S} \quad (32)$$

Where:

$V_n$ : The rms voltage across a winding.

N: Turn number of the coil.

B: The magnetic field peak amplitude.

f: the voltage frequency applied to the winding.

S: the section of one limb magnetic circuit

Sheet of steel used in simulation:

Steel material used: AISI 1010

Coefficients of iron losses in the model Bertotti:

Hysteresis:  $KH = 15,45 \cdot 10^{-3} [SI]$ .

Additional:  $KE = 3,2 \cdot 10^{-3} [SI]$ .

Resistivity:  $17,6 \cdot 10^8 [\Omega]$ .

Thickness of sheet metal:  $0,5 \cdot 10^{-3} [m]$ .

Density:  $7,85 \cdot 10^3 [kg/m^3]$ .

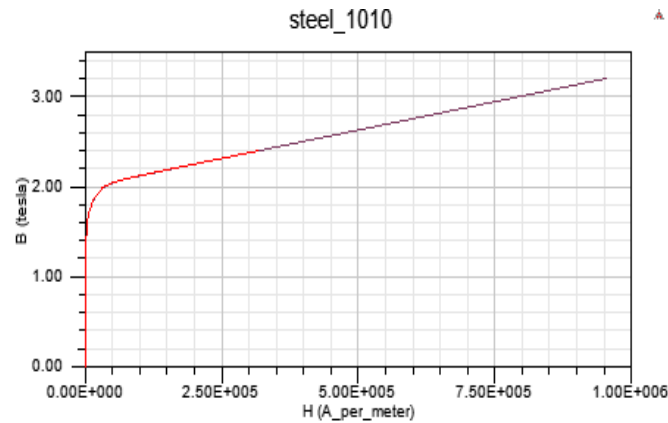


Fig. 5 BH Steel 1010 characteristics

TABLE III  
WINDING PARAMETERS AND COILS TURN NUMBER

	Voltage (V)		Turns number	section
	Coil	Value		
Primary winding	Coil_A1	62	97	1.32cm <sup>2</sup>
	Coil_A2	338	528	1.32cm <sup>2</sup>
	Coil_A3	400	625	1.32cm <sup>2</sup>
Secondary winding	Coil_A4	117	187	1.50cm <sup>2</sup>
	Coil_A5	117	187	1.50cm <sup>2</sup>

#### IV. 2D, 3D MODELING OF THE PROPOSED AUTOTRANSFORMER

In transformers, finite element method can be used to calculate the following quantities [9]:

- Magnetic field analysis
- Eddy currents and winding stray losses

- Leakage inductance
- Short-circuit impedance

This work present the geometric design for resulting the flux density 'B', the field density 'H', current density 'J' and the flux line 'A' in the autotransformer with 40° phase shifting.

#### A. Geometry Design

Before entering the actual constructing step, the type of analysis should be noted, in this paper we used the transient magnetics problems characteristic magnetic field sizes vary with time. The geometric structure of the model shall be established from a preliminary design by standard methods or existing physical model. Input data (Core size, Coil size) shown in Table 2 and Table 3 may be entered numerically, in which case it follows a fixed pattern, either parametric form, in this case the geometry of the transformer with core simplified in order to reduce the complexity. We can bring the geometries directly and simplified it inside Maxwell. This solution, whereas initially more time-consuming, statement is preferable to a certain configuration optimization. At this step are defined regions that it is to be assigned different material properties [12].

TABLE II  
PARAMETERS YOKE

Name	Value	Unit	Evaluated Value	Description
Dia Leg	40	mm	40mm	Outer diameter of leg cross section
Dist Leg	80	mm	80mm	Leg center to center distance
Dist Yoke	160	mm	160mm	Yoke center to center distance
Stages	40		40	Number of stages of leg cross-section
Width Yoke	40	mm	40mm	Yoke width

TABLE II  
PARAMETERS COIL

Name	Value	Unit	Evaluated Value	Description
Dist Leg	80	mm	80mm	Leg center to center distance
Coil Type	1		1	Coil type: 1 for solenoid coil; 2 for pancake coil
Width In	41	mm	41mm	Coil width between tow inner sides
Depth In	41	mm	41mm	Coil depth between two inner ends
Radius In	30	mm	30mm	Coil inner fillet radius
Thick Coil	2	mm	2mm	Coil thickness of one side
High Coil	119	mm	119mm	Coil height

#### B. Mesh Operations

When the geometry is prepared, it is then divided in to small finite elements [11]. The size of each mesh or element consists in dividing the field of study in geometry characterized by the presence of specific points, called nodes. The most elements geometric used are the triangle nodes are placed in three corners of its Fig. 6.

Usually the meshing operation is automatic, with network generator included in the program.

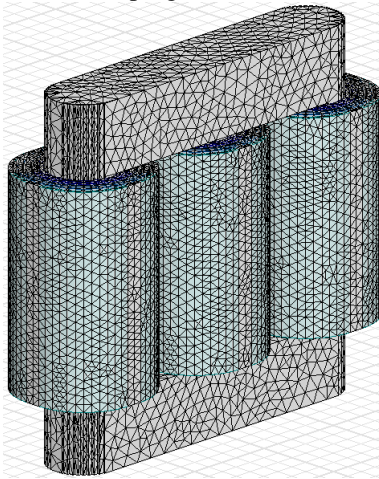


Fig. 6 3D meshing results of the autotransformer

### V. RESULT AND DISCUSSION

The proposed delta connected autotransformer based an 18-pulse converter is modelled and designed for resistive load and validated with an experimental prototype realized in the laboratory MMA shown in Fig. 7.

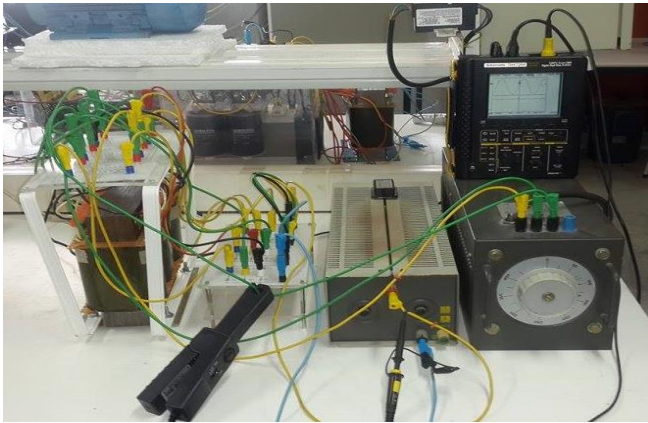


Fig. 7 Experimental realization of the Delta-connected autotransformer based 18 pulse ac-dc converters

The topology of 18-pulse ac-dc converters illustrated in Fig. 8 (a) gives an output continuous voltage with fewer ripples in the waveform. Moreover, between 0.02s and 0.04s, means that during 20ms we can view the 18 undulations which is provided by this topology means three times of six pulse configuration. These results are validated by the experimental finding in Fig. 10 (a) which gives an output voltage and an output current closer to the continuous signal.

The waveform of input current shown in Fig. 8 (b) is clear sinusoidal and improves harmonics in network side. Then it's validated by the experimental outcomes shown in Fig. 10 (b).

The total harmonic distortion "THD" of the input current in network side shown in Fig. 9 is with THD current = 7.98%, then this connection of autotransformer capable to suppress harmonic up to 13<sup>th</sup> and minimize the THD of the source current.

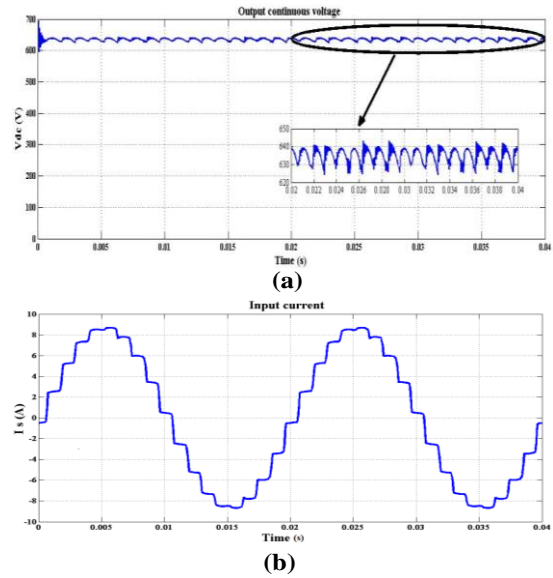


Fig. 8 (a) Simulated waveforms of Output voltage of auto transformer for 18-Pulse ac-dc converter; (b) Simulated waveforms of input current

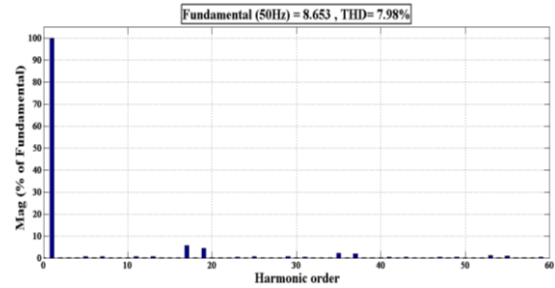


Fig. 9 THD of input current

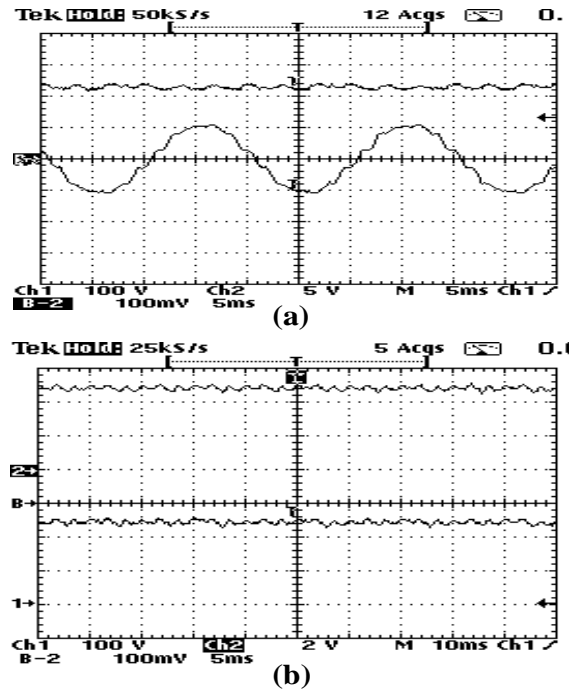


Fig. 10 (a) Experimental results of the output voltage and the ac current; (b) Experimental results of the output voltage and output current

The use of a magnetic core can enormously concentrate the strength and increase the effect of magnetic fields produced by electric currents. The properties of a device will depend crucially on the following factors:

- The geometry of the magnetic core.
- The amount of air gap in the magnetic circuit.
- The proprieties of the core material
- The operating temperature of the core.
- Whether the core is laminated to reduce eddy currents.

The uniform flux density 'B' distribution in the iron core as shown in Fig. 11 (a), represent a healthy magnetic circuit, the color represents the amplitude of the magnetic flux , red being high amplitude . Fig. 11 (b) shows the field intensity 'H' between primary and secondary windings. The current density 'J' is presented in Fig. 11 (c). Fig. 11 (d) presents the line flux of the autotransformer and is clear that it is completely concentrated in the iron core.

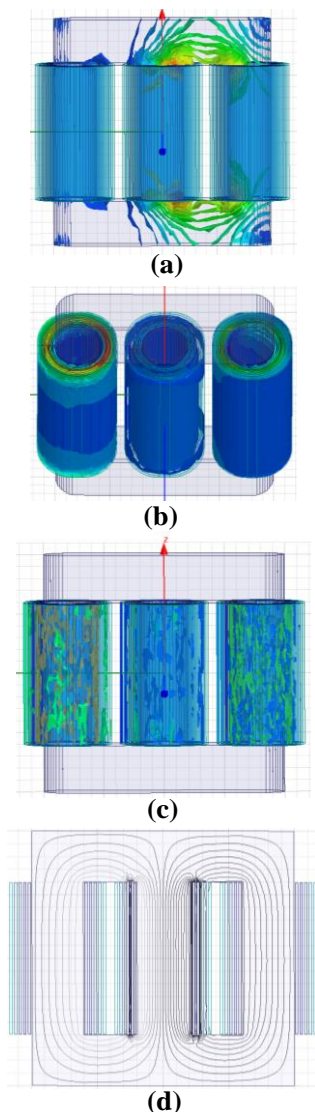


Fig. 11 (a) 3D Magnetic flux B (b) 3D Magnetic flux H (c) 3D current density (d) 2D Flux lines

## VI. CONCLUSIONS

The simulation results shows that the proposed Delta-connected autotransformer have a great advantage. Indeed this design offers a best quality of output current and voltage compared with the two configurations 6-pulse and 12-pulse. This design proves the elimination of the harmonic with order 5<sup>th</sup>, 7<sup>th</sup>, 11<sup>th</sup> and 13<sup>th</sup>. Then, the magnetic field analysis (the flux density, the field density, the current density and flux lines) of power transformer are presented using the Maxwell ANSYS 2D and 3D software, the results show the validity of this program and present the healthy magnetic circuit of the proposed autotransformer. Finally, Future works will focus on other simulation for the circuit equivalent calculation (leakage inductance and short circuit impedance), in addition on other topologies who give better THD coefficient such as another design of auto-connected with another special coupling and topologies of 24 pulses.

## REFERENCES

- [1] *IEEE Standard, 519. (1992) "IEEE Recommended Practices and Requirements for Harmonics control in Electric Power Systems"*.
- [2] B.A. Arafet and B.A. Faouzi, "Delta-Connected Autotransformer Based 18 Pulse AC-DC Converters," *2<sup>nd</sup> International Conference on Automation, Control, Engineering and Computer Science ACECS Sousse, Tunisia, march 22-24, 2015.*
- [3] B. Singh, G. Bhuvaneswari and V. Garg, "Harmonic mitigation using 12-pulse AC-DC converter in vector-controlled induction motor drives," in *Power Delivery, IEEE Transactions on*, vol.21, no.3, pp.1483-1492, July 2006.
- [4] R. Agarwal, S. Singh, "Harmonic mitigation in voltage source converters based HVDC system using 12-pulse AC-DC converters," in *India Conference (INDICON), 2014 Annual IEEE*, vol., no., pp.1-6, 11-13 Dec. 2014.
- [5] B. Singh, G. Bhuvaneswari and R. Kalpana, "Autoconnected transformer-based 18-pulse ac-dc converter for power quality improvement in switched mode power supplies," *Power Electronics, IET*, vol.3, no.4, pp.525-541, July 2010.
- [6] K. Oguchi, "Autotransformer-based 18-pulse rectifiers without using dc-side interphase transformers: Classification and comparison," *International Symposium Power Electronics, Electrical Drives Automation and Motion SPEEDAM*, pp.760-765, June 2008.
- [7] J.V. Leite, A. Benabou, S N. adowski and M.V.F.da Luz, "Finite Element Three-Phase Transformer Modeling Taking Into Account a Vector Hysteresis Model," in *Magnetics, IEEE Transactions on*, vol.45, no.3, pp.1716-1719, March 2009.
- [8] I. Hernández, F. de León, J.M. Cañedo and J.C. Olivares-Galván, "Modelling transformer core joints using gaussian models for the magnetic flux density and permeability," in *Electric Power Applications, IET*, vol.4, no.9, pp.761-771, Nov. 2010.
- [9] A. Ahmad, I. Javed, W. Nazar, "Short Circuit Stress Calculation in Power Transformer Using Finite Element Method on High Voltage Winding Displaced Vertically," *International Journal of Emerging Technology and Advanced Engineering*, Volume 3, Issue 11, November 2013.
- [10] J. Faiz, B.M. Ebrahimi, T. Noori, "Three- and Two-Dimensional Finite-Element Computation of Inrush Current and Short-Circuit Electromagnetic Forces on Windings of a Three-Phase Core-Type Power Transformer," in *Magnetics, IEEE Transactions on*, vol.44, no.5, pp.590-597, May 2008.
- [11] J. Schöberl, "An advancing front 2D/3D-mesh generator based on abstract rules," *Computing and Visualization in Science* Vol. 1, Issue 1, pp 41-52, February 1997.
- [12] M. Mohan and P. K. Singh, "Distribution Transformer with Amorphous-CRGO Core: An Effort to Reduce the Cost Of Amorphous Core Distribution Transformer" *ARPJ Journal of Engineering and Applied Sciences*, Vol. 7, No. 6, June 2012.